

# Fatigue Endurance Investigation of Post-processed Surfaces of L-PBF Ti-6Al-4V under Flexural Stress

C. Banuelos<sup>1,2\*</sup>, B. Ramirez<sup>1,2</sup>, A. De la Cruz<sup>1,2</sup>, S. T. Nabil<sup>1,2</sup>, E. G. Arrieta<sup>1,2</sup>, R. B. Wicker<sup>1,2</sup>,  
and F. Medina<sup>1,2</sup>

<sup>1</sup> Department of Aerospace and Mechanical Engineering, University of Texas at El Paso, El Paso, TX 79968, USA;

<sup>2</sup> W.M. Keck Center for 3D Innovation, El Paso, TX, USA;

\* Corresponding author ([cbanuelos4@miners.utep.edu](mailto:cbanuelos4@miners.utep.edu))

## Abstract

Numerous research works can be found focusing on fatigue properties of AM components, however most of this literature is focused on uniaxial testing. Because the very few actual components under uniaxial loading conditions found in any application, it is also important to investigate fatigue performance under loads that produce combined stresses, such as bending. This project investigates the fatigue endurance of LPBF Ti-6Al-4V specimens subjected to four different surface finishing post-processes (milled, ground, polished and abrasive media). The test consisted of a force-controlled cyclic load applied on the specimen in a 4-point bending setup until fracture. The study incorporated mechanical and optical techniques to measure and quantify the characteristic surface roughness of the post-processes. Additionally, failure mechanisms are discussed on fractographs. The data analyses suggested that internal defects commonly present in additively manufactured parts had a more significant impact on the fatigue life than surface roughness of post-processed parts.

## Introduction

Additive manufacturing, commonly known as 3D printing, is a groundbreaking technology that enables the fabrication of intricate parts and objects by layer-by-layer construction of materials. Laser Powder Bed Fusion (LPBF) is one of the most popular and versatile additive manufacturing techniques. It involves utilizing a high-powered laser to selectively melt and fuse metal or plastic powder, resulting in the desired shape formation. LPBF finds extensive applications in industries such as aerospace, automotive, medical, and consumer goods due to its ability to produce highly precise and customized parts [1-3].

The focus of interest in this study lies in the manufacturing of aerospace-grade titanium alloy (Ti-6Al-4V) using LPBF. This material possesses numerous advantages, including lightweight properties and high strength. However, the LPBF process introduces certain drawbacks, such as residual stresses and poor surface finish. These factors can adversely affect the mechanical performance and fatigue life of the manufactured parts [4,5]. Various post-processing techniques, including heat treatments and machining methods, can be employed to mitigate these

disadvantages. However, it is important to note that these processes often come with added costs and delays in the supply chain.

Previous research studies [6-8] have demonstrated a correlation between surface quality and fatigue performance under cyclic loading. An inadequate surface finish creates imperfections that lead to stress concentration, ultimately causing the part to fail. In the context of this research, poor surface finish can serve as initiation sites for crack growth, leading to reduced fatigue performance.

The objective of this study is to evaluate the impact of surface finish on the performance of additively manufactured parts and quantify the extent to which bending fatigue life can be enhanced. Additionally, the study aims to determine if specific post-processing techniques offer significant advantages over others in terms of improving fatigue performance.

## **Methods**

### **Powder characterization**

The specimens used in this research were manufactured using grade 5 titanium alloy powder. The powder was sampled according to ASTM B215-15 standard [9] and was then characterized by a Retsch Technology Camsizer X2 X-Dry as per ASTM B822 standard [10].

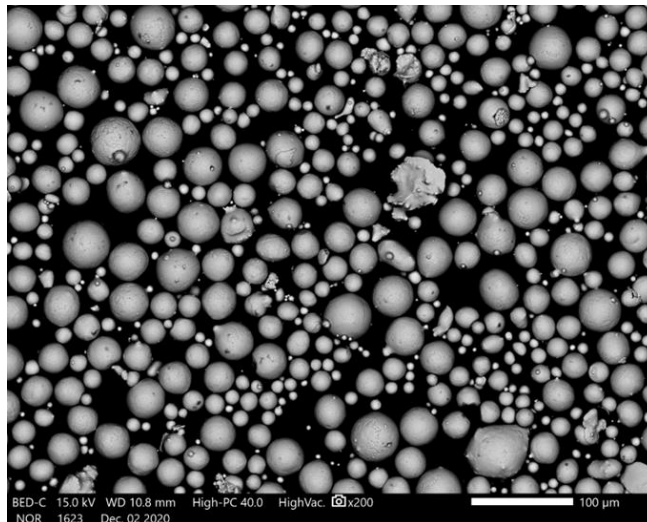


*Figure 1: SEM image of Ti-6Al-4V powder*

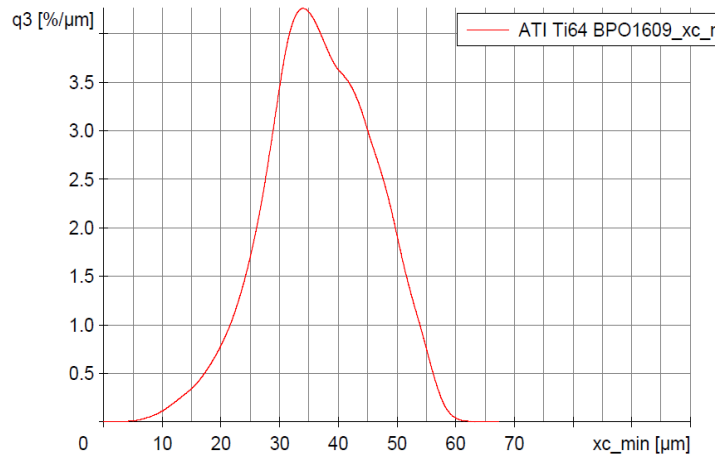


Figure 2: Powder size distribution graph

### EOS build parameters

The specimens were built in an EOS M290 laser powder bed fusion system equipped with two Ytterbium lasers in an Argon environment. All samples were built using EOS Nominal parameters; that is a laser power of 280 W at a scanning speed of 1200 mm/s. These parameters are located within the process window as demonstrated in Figure 4 below.



Figure 3: Image of EP08 samples on build plate

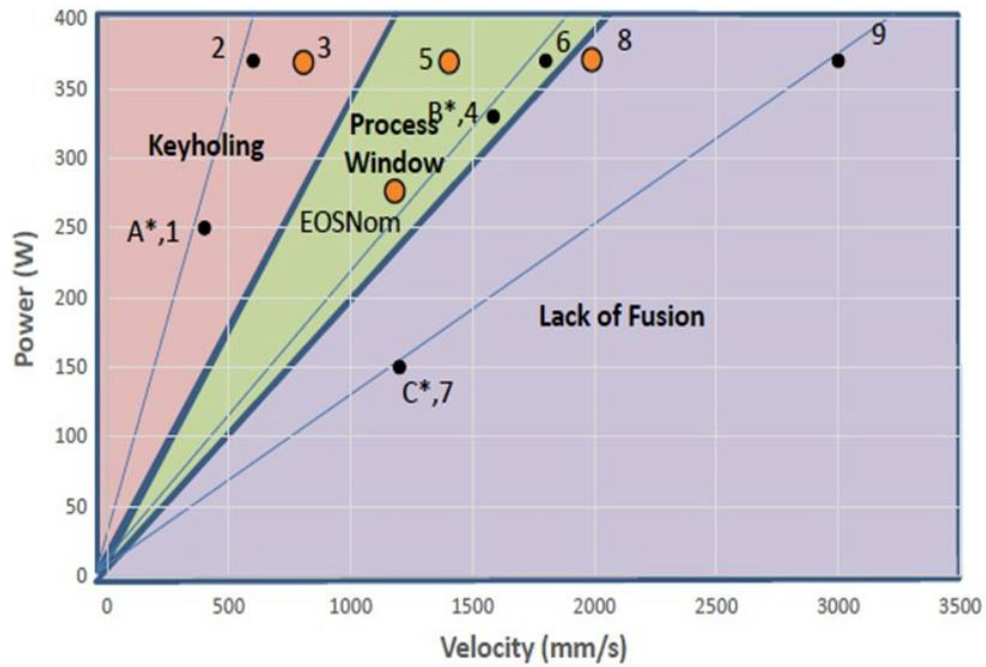


Figure 4: P-V diagram of the process regions of grade 5 titanium for L-PBF

### Heat treatment

The parts were stress relieved to remove any internal thermal stress commonly associated with the laser powder bed process. The stress relief was achieved by allowing the parts to evenly heat up to 600°C and then evenly cool down to room temperature in a vacuum furnace at a ramp and cooling rate of 5°C/min.

### Sampling and test development

The parts were then randomly assigned into the different machining strategies as well as designated toward developing the test design. Furthermore, the machined samples were allocated into four different maximum stress levels (667 MPa, 900 MPa, 1067 MPa, and 1200 MPa) for testing and three samples from each machining technique were set aside as spares as shown in Table 1. Figure 5 illustrates the print location of the samples and how they were randomly assigned to the different surface finishes.

Table 1: Test Matrix

Machining Method	1200 MPa	1067 MPa	900 MPa	667 MPa	Spares	Total
Tangential Milling	3	3	3	3	3	15
Deci Duo	3	3	3	3	3	15
Surface Ground	3	3	3	3	3	15
LTI Polished	3	3	3	3	3	15
<b>Total</b>	12	12	12	12	12	60

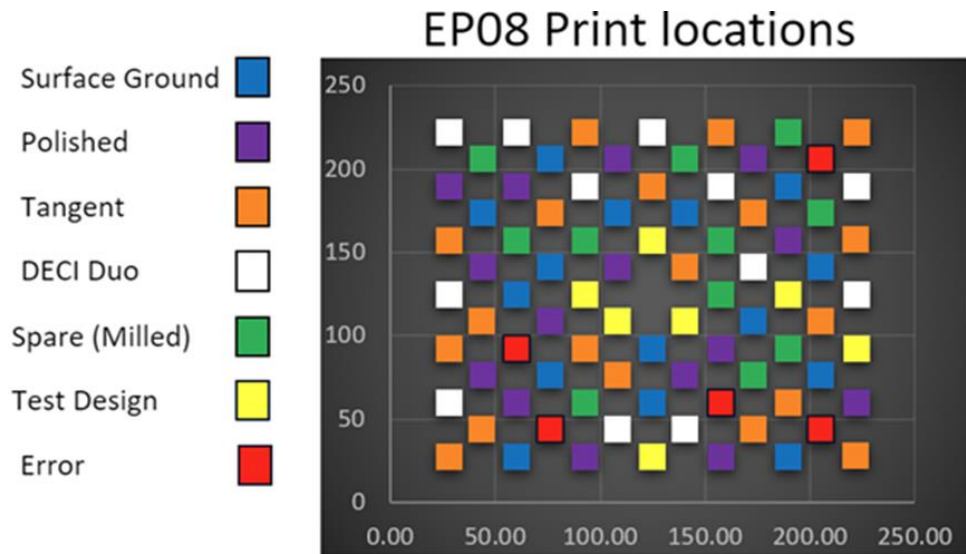


Figure 5: Map of sample assignments according to their build plate print location.

## Machining techniques

Four different machining techniques were explored in this project, the first of which was a thermal atomized fusillade performed on a Deci Duo machine by Post Process. The intent of this process is to reduce the processing time of AM parts by streamlining the steps from finished print to finished product. This method works by allowing a combination of detergent, abrasive media, water, and air to be shot out of nozzle as the sample rotates to improve the surface quality. Figure 6 illustrates how the surface of these samples looked once completed. Figure 7 demonstrates how the specimens were setup and the parameters used for this process.



Figure 6: Image of finished Deci Duo sample

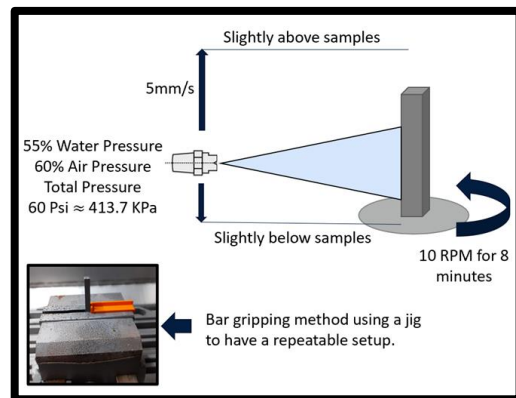


Figure 7: Illustration of Deci Duo process

The second machining technique was tangential milling. This process consisted of utilizing a half inch cutter to remove 0.5-mm of material from each side in a single pass. Figures 8 and 9 show the surface of the milled sample and a visualization of how the samples were machined, respectively.

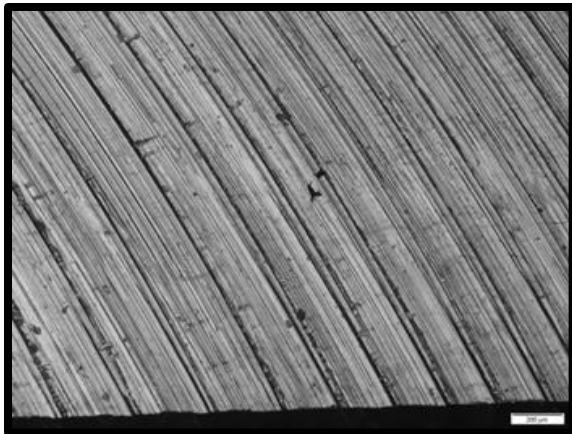


Figure 8: Image of finished tangential milled sample

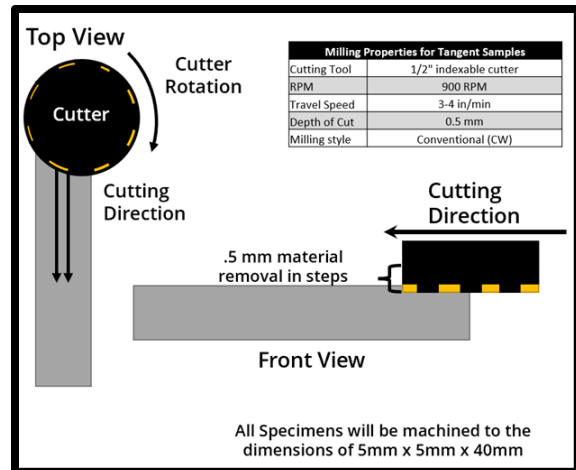


Figure 9: Illustration of milling process.

The previous methods were performed at UTEP with the milling able to be done at any machine shop. The third machining technique was commissioned to a local shop and consisted of using a grinding wheel in a back-and-forth motion to remove 0.5-mm of material from each side. Figure 11 illustrates how this third process was completed according to the vendor's process specifications. Figure 10 demonstrates how the surface of the ground samples looked; scratches can be seen overlapping along the longitudinal axis of the specimen.

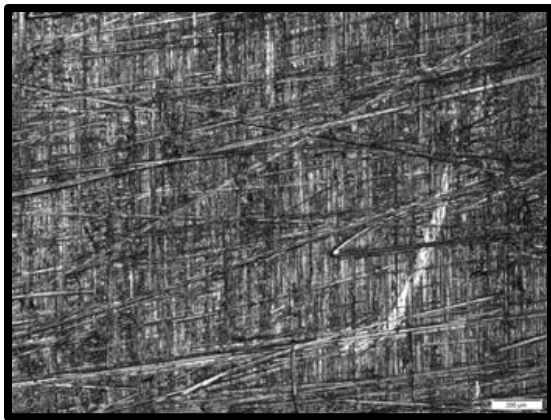


Figure 10: Image of finished surface ground sample

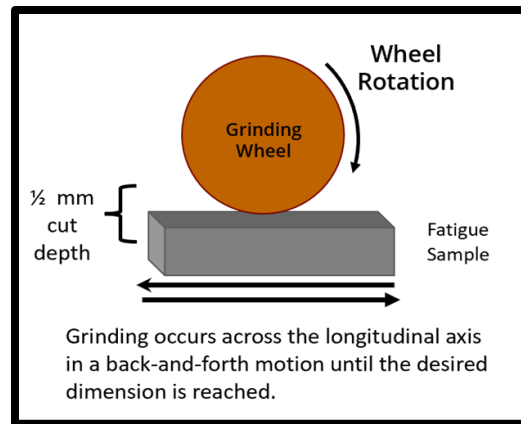
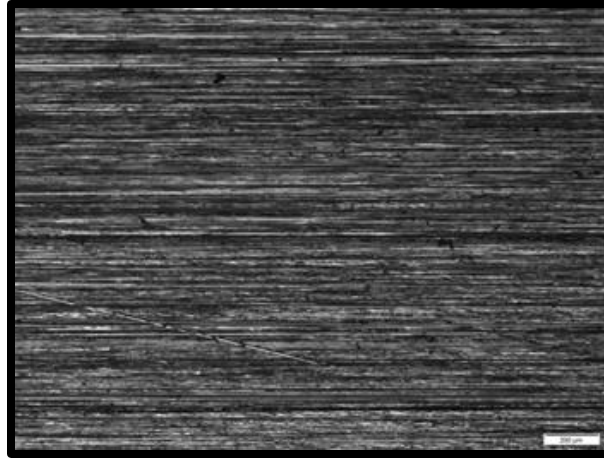


Figure 11: Illustration of grinding process.

The final machining method was also performed by a vendor, Laboratory Testing Incorporated (LTI). The samples were polished and although the company did not provide much information on how the samples were to be polished, it is important to note that the company is an industry certified and accredited site for machining and testing a wide variety of materials. LTI also guaranteed the polished samples have an average line roughness ( $R_a$ ) of less than or equal to 0.8 microns. Figure 12 below shows the finished surface of these samples observed under a microscope. Scratches can also be seen however these are much more uniform throughout the sample.



*Figure 12: Image of polished sample*

### **Surface quality inspection**

Line roughness measurements were taken for all the samples using a mechanical profilometer (Mitutoyo Surftest SJ-210) and optical microscope (Keyence VR-5000) to determine the surface quality that each machining technique produced. The technique that produced the highest roughness values would be considered the worst surface quality and vice versa.

### **Mechanical Testing**

An MTS Landmark machine equipped with a 100 kN load cell was utilized to conduct 4-point bending fatigue testing. The testing procedure involved employing two fixtures to establish four-pin connections on the sample, with two pins positioned on the top and two on the bottom. The alignment of the pins ensured an inner span of 10 mm and an outer span of 30 mm on the respective surfaces (loading side) of the sample. The fatigue test was designed to subject the samples to cyclical loading at a stress ratio of 0.1 and a frequency of 10 Hz until failure occurred. To prevent excessive testing duration, a test would be terminated automatically if it reached  $7 \times 10^6$  cycles, thereby qualifying as runoff.

### **Fracture Surface Analysis**

To gain a deeper understanding of the failure mechanism exhibited by the samples, the fracture surface analysis was conducted employing a Keyence VHX optical microscope. To facilitate this analysis, the samples underwent a series of isopropanol and acetone baths in an ultrasonic cleaner to effectively eliminate any oils or impurities that might have been present during testing. Following the cleaning process, the fracture surface of the samples was meticulously examined using the VHX microscope. Multiple images were captured to facilitate the identification of the fracture origin. Additionally, the samples were classified based on the specific location of the fracture, namely surface, chamfer, or internal defect.

## Results and Discussion

As demonstrated in Table 2 below the average line roughness for all the samples according to their respective surface finishing were recorded. It can be noted that there is a significant improvement in roughness when employing any post processing on the parts. This is illustrated in the vast difference in roughness values between an as built sample and any of the machined samples. Furthermore, it is important to note that when the maximum profile valley depth ( $R_v$ ) values are compared, the ranking of surface quality from best to worst is: LTI polished, surface ground, tangential milling, Deci Duo, and as built.

**Table 2: Average Line Roughness for each Machining Technique**

Machining Method	Average $R_a$ ( $\mu\text{m}$ )	Average $R_v$ ( $\mu\text{m}$ )
As Built	22.51	48.17
LTI Polished	0.164	.544
Surface Ground	0.440	1.737
Tangential Milling	1.101	3.167
Deci Duo	1.041	4.112

The raw fatigue data was used to generate figure 13 below comparing the performance of the samples based on the different surface finishes. The data for the machined samples are clustered together with the Deci Duo and milled samples having a slightly better performance over the surface ground and polished samples. Additionally, the performance of all machined samples is vastly superior to that of as built samples, as none of the latter ever achieved runoff, even at significantly lower stress levels.

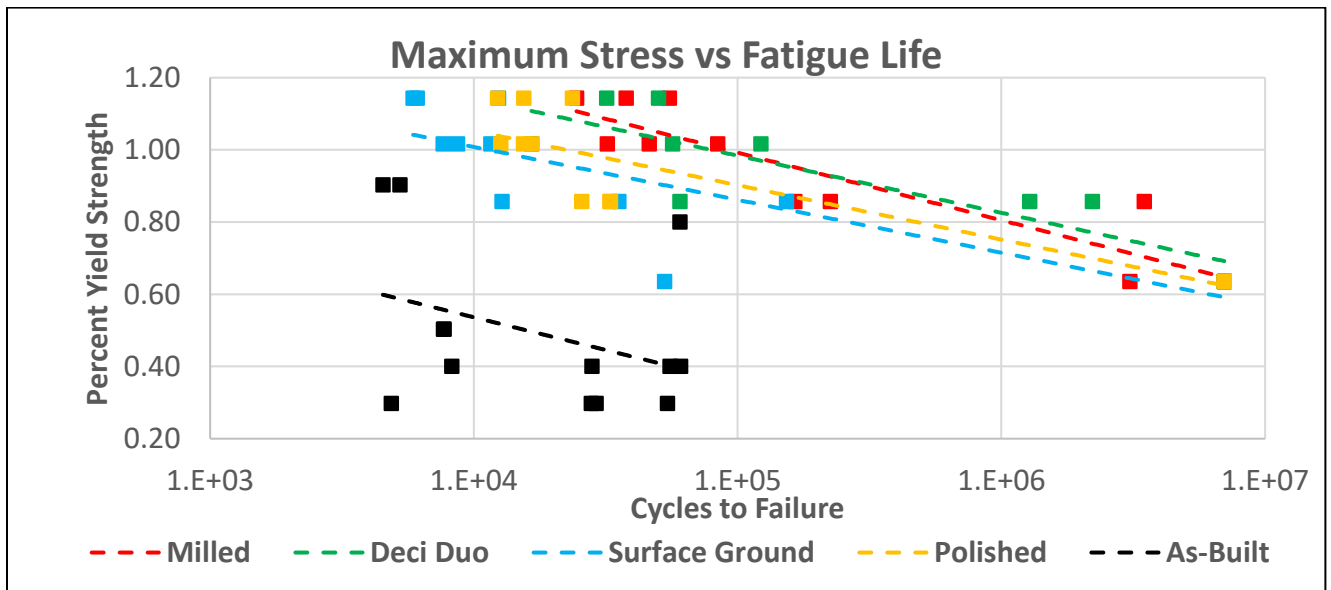


*Figure 13: Percent Yield Strength vs. Cycles to Failure Graph*

The graph suggests that the two worst machining methods may improve the fatigue life of the samples, however this cannot be the case. To further understand why the data suggests this, the failure mechanisms of each sample were observed. Figures 13, 14, and 15 demonstrate that there were three crack initiation sites: initiation at the surface, at the chamfer, and at an internal defect. Table 3 further suggests that there exists a trend in the fatigue life relative to where the crack initiated. That is that when the crack initiates from the surface, the fatigue life is shorter and when the initiation point is at an internal defect, the fatigue life is longer. This makes sense; the surface receives stress concentrations much sooner than the chamfer or any internal defect therefore leading to a lower fatigue life.

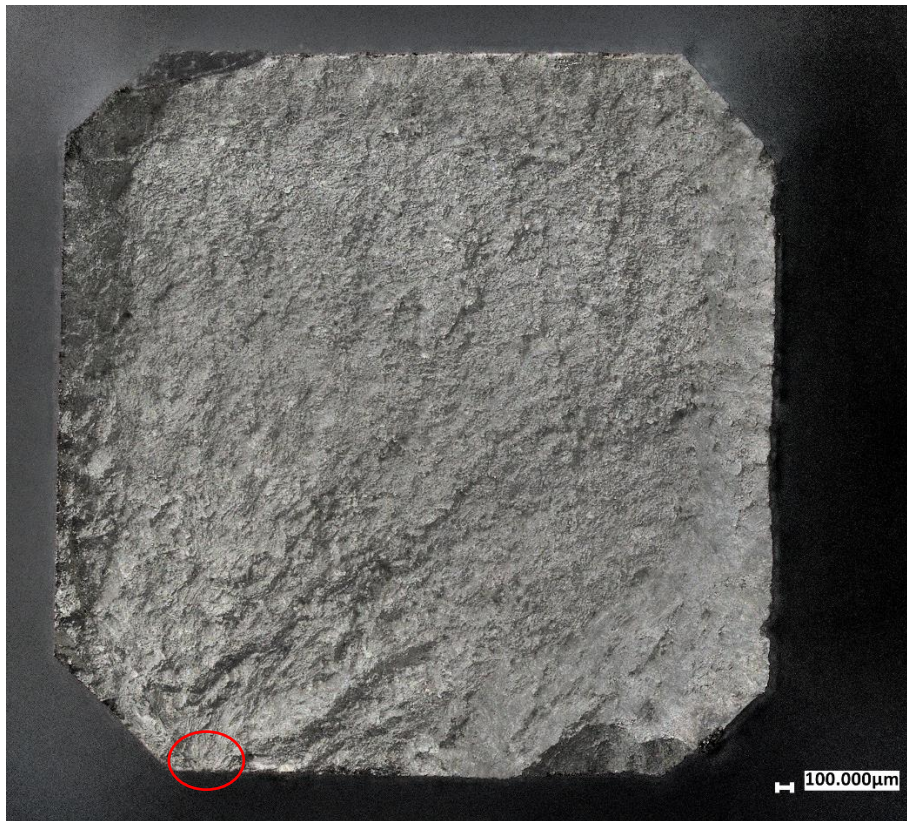


*Figure 14: Sample F17 – Initiation site on the lower left side near the chamfer*



*Figure 15: Sample F49 - Initiation site on the lower left side chamfer*



*Figure 16: Sample F77 - Initiation site at defect on the lower right side*

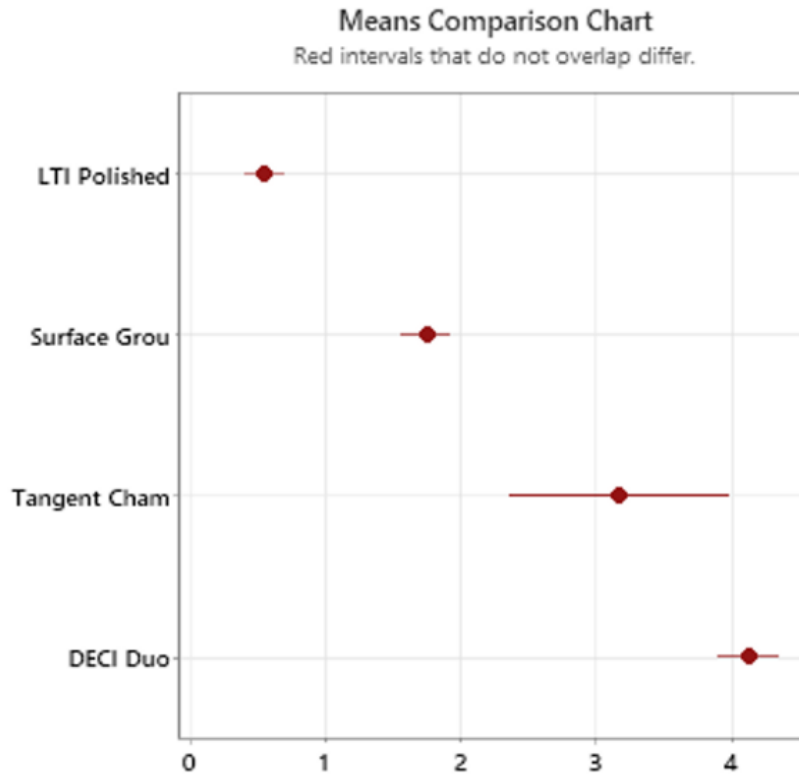
**Table 3: Fracture Initiation Site and Average Fatigue Life**

Machining Technique	Initiation Site	Count	Average Fatigue Life
Tangential Milling	Surface	1	37,852
	Chamfer	5	48,421
	Defect	4	1,735,574
Surface Ground	Surface	9	17,046
	Chamfer	1	153,446
	Defect	0	-
Deci Duo	Surface	5	55,501
	Chamfer	0	-
	Defect	4	1,185,435
LTI Polished	Surface	4	14,259
	Chamfer	5	26,104
	Defect	0	-

However, this correlation between the fracture initiation site and the fatigue life of the corresponding sample, also does not explain the dilemma observed in figure 13. In fact, the same trend of the specimens with better surface finishes having lower fatigue life is further seen when the data is isolated to only include the samples that failed from the surface.

To understand the significance of this relationship two statistical tests were performed on Minitab, a statistical analysis software. The first test was an analysis of variance (ANOVA) amongst the different machining techniques. This was done to see if there was a statistically significant difference between the four processes. Figure 17 demonstrates that the surface ground and polished samples were unique from the other samples and that the milled and Deci Duo samples were like one another due to an overlap in their mean roughness values.

Furthermore, the fatigue data and  $R_v$  measurements were set to fit a general linear model. The null hypothesis of this test is that there exists no significant correlation between the variables. This hypothesis can be rejected when the P-value of the test is less than 0.05, which indicates a confidence interval of 95 percent. The variables explored for this test were the fatigue life (cycles) versus the machining techniques and the stress levels. This was done to understand if one or both the machining and/or stress levels had a significant impact on the fatigue life of the samples. Figure 18 demonstrates the results of this test: only the testing stress had a significant impact on the fatigue life of the specimens.



**Which means differ?**

#	Sample	Differs from
1	LTI Polished	2 3 4
2	Surface Grou	1 3 4
3	Tangent Cham	1 2
4	DECI Duo	1 2

Figure 17: ANOVA results comparing the line roughness values of the different machining techniques.

## Analysis of Variance

Source	DF	Adj SS	Adj MS	F-Value	P-Value
Machining	3	4.42698E+12	1.47566E+12	0.92	0.439
Stress	3	2.83068E+14	9.43559E+13	58.98	0.000
Error	39	6.23875E+13	1.59968E+12		
Lack-of-Fit	9	1.03282E+13	1.14757E+12	0.66	0.736
Pure Error	30	5.20594E+13	1.73531E+12		
Total	45	3.48437E+14			

Figure 18: General Linear Model: Cycles versus Machining, Stress results

## **Conclusions**

In conclusion, it was observed that machining laser powder bed fusion parts significantly improves fatigue life when comparing the performance of as built samples. In this study, it was also found that machining technique had no significant correlation to the fatigue life of the specimens, but rather the maximum testing stress would be the deciding factor when predicting fatigue performance. This could be the case for specimens below a certain line roughness threshold such as in this study where all machined samples had an  $R_v$  and  $R_a$  of less than 5 and 2 microns, respectively. Another explanation could also be attributed to stresses introduced during the post processing. Further work needs to be completed to understand which is the case. Additionally, it is worth noting that achieving satisfactory results may not require surface quality improvement beyond the capabilities of simple milling techniques.

## **Acknowledgements**

The research described here was performed at The University of Texas at El Paso (UTEP) within the W.M. Keck Center for 3D Innovation (Keck Center). The authors would also like to thank Enrique Garibay and Hunter Taylor for their assistance in the machine setup and the manufacturing of the samples. Primary support for this research was provided by grant number 1110234-424023 from NASA ULI as well as strategic investments via discretionary UTEP Keck Center funds and the Mr. and Mrs. MacIntosh Murchison Chair I in Engineering Endowment at UTEP. The views and opinions expressed in this article are those of the authors and do not necessarily reflect the official opinion or policy of NASA ULI or of any agency of the US government.

## References

- [1] ASTM F2792-12a, "Standard Terminology for Additive Manufacturing Technologies," ASTM International, 2012
- [2] N. Guo and M. C. Leu, "Additive manufacturing: technology, applications and research needs," *Front. Mech. Eng.*, vol. 8, no. 3, pp. 215–243, Sep. 2013, doi: 10.1007/s11465-013-0248-8.
- [3] L. Thijs, F. Verhaeghe, T. Craeghs, J. V. Humbeeck, and J.-P. Kruth, "A study of the microstructural evolution during selective laser melting of Ti–6Al–4V," *Acta Materialia*, vol. 58, no. 9, pp. 3303–3312, May 2010, doi: 10.1016/j.actamat.2010.02.004.
- [4] P. Mercelis and J. Kruth, "Residual stresses in selective laser sintering and selective laser melting," *Rapid Prototyping Journal*, vol. 12, no. 5, pp. 254–265, Jan. 2006, doi: 10.1108/13552540610707013.
- [5] J. Gockel, L. Sheridan, B. Koerper, and B. Whip, "The influence of additive manufacturing processing parameters on surface roughness and fatigue life," *International Journal of Fatigue*, vol. 124, pp. 380–388, Jul. 2019, doi: 10.1016/j.ijfatigue.2019.03.025.
- [6] L. Denti, E. Bassoli, A. Gatto, E. Santecchia, and P. Mengucci, "Fatigue life and microstructure of additive manufactured Ti6Al4V after different finishing processes," *Materials Science and Engineering: A*, vol. 755, pp. 1–9, May 2019, doi: 10.1016/j.msea.2019.03.119.
- [7] J. Pegues, M. Roach, R. Scott Williamson, and N. Shamsaei, "Surface roughness effects on the fatigue strength of additively manufactured Ti-6Al-4V," *International Journal of Fatigue*, vol. 116, pp. 543–552, Nov. 2018, doi: 10.1016/j.ijfatigue.2018.07.013.
- [8] L. Ednie et al., "The effects of surface finish on the fatigue performance of electron beam melted Ti–6Al–4V," *Materials Science and Engineering: A*, vol. 857, p. 144050, Nov. 2022, doi: 10.1016/j.msea.2022.144050.
- [9] ASTM B215-15, "Standard Practices for Sampling Metal Powders," ASTM International, 2015.
- [10] ASTM B822-20, "Standard Test Method for Particle Size Distribution of Metal Powders Using Semiautomatic Analytical Electrozone Separation," ASTM International, 2020